Rotational dynamics of proteins from spin relaxation rates and molecular dynamics simulations

O. H. Samuli Ollila*
Insititute of Biotechnology, University of Helsinki
(Dated: May 15, 2017)

I. INTRODUCTION

Protein conformational sampling and entropy plays significant role in protein functionality and interactions with other biomolecules. The related Protein backbone and side chains dynamics as well as protein overall brownian tumbling can be experimentally studied by using NMR relaxation experiments of backbone N-H or side chain ?? bonds [1–3]. Spin relaxation data is usually analyzed by describing the sampled bond orientations with order parameter S^2 respect to the protein reference frame and assuming that overall and internal motions are independt [2**?**]. Order parameters and timescales for overall and internal motions can be then extracted by fitting various functional forms to spin relaxation data measured with different magnetic field strengths [1, 2].

This approach has been successfully applied for large amount of proteins with isotropic shape and overall rotational diffusion [1]. The resulting order parameters and overall rotational diffusion coefficients have been used in wide range applications, including analysis of conformational entropy [**?**], binding entropy of ?? [**?**], resolving sampled structures [**?**] and validating molecular dynamics simulations [**?**]. On the other hand, segmental level information has been used in validation and improvement of molecular dynamics simulation force fields [**?**]. Segmental order has been also related to conformational entropy of proteins [**?**].

Spin relaxation rates are typically intepreted by using various dynamical models assuming different level of complexity of rotational relaxation processes. The most simplistic models assume single timescale and order parameter for internal motion and isotropic overall rotational diffusion. However, biomolecules often experience anisotropic overall diffusion and several internal timescales. Models for more complicated models have been also introduced, however, there are more fitting parameters in these models and intepretation of experiments becomes extensively difficult.

Classical molecular dynamics simuations contain, in principle, all the complexity of the timescales and could be used to interpret the rotational dynamics measured with spin relaxation experiments. However, this has not been a trivial task due to the force field issues and limited available time scales in the simulations.

In this work we present approach that can be used to analyze spin relaxation experiments by using classical molecular dynamics simulations. The approach can be used for anisotropic molecules and allows a correction of anisotropic overall diffusion. We demonstrate the usage of the approach for two aniotropic protein constructs from engineered from Helicobacteri pyroli and Pseudomonas.

II. METHODS

A. Spin relaxation and rotational dynamics of molecules

Spin relaxation rates R_1, R_2 and R_{NOE} measured from NMR experiments for N-H bondsare related to the molecular dynamics through spectral density $J(\omega)$ and equations [4, 5]

$$R_1 = \frac{d_{\mathrm{NH}}^2 N_{\mathrm{H}}}{20}\Big[J(\omega_{\mathrm{H}}-\omega_{\mathrm{N}}) + 3J(\omega_{\mathrm{N}}) + 6J(\omega_{\mathrm{N}}+\omega_{\mathrm{H}})\Big] + \frac{(\sigma\omega_{\mathrm{N}})^2}{15} j(\omega_{\mathrm{N}}), \tag{1}$$

$$R_2 = \frac{1}{2}\frac{d_{\mathrm{NH}}^2 N_{\mathrm{H}}}{20}\Big[4J(0) + 3j(\omega_{\mathrm{N}}) + J(\omega_{\mathrm{H}}-\omega_{\mathrm{N}}) + 6J(\omega_{\mathrm{H}}) + 6J(\omega_{\mathrm{N}}+\omega_{\mathrm{H}})\Big] + \frac{(\sigma\omega_{\mathrm{N}})^2}{15*6}[4J(0)+3J(\omega_{\mathrm{N}})], \tag{2}$$

$$R_{\mathrm{NOE}} = 1 + \frac{d_{\mathrm{NH}}^2 N_{\mathrm{H}}}{20}\Big[6J(\omega_{\mathrm{N}}+\omega_{\mathrm{H}}) + J(\omega_{\mathrm{H}}-\omega_{\mathrm{N}}))\Big]\frac{\gamma_{\mathrm{H}}}{\gamma_{\mathrm{N}} R_1}, \tag{3}$$

where ω_{N} and ω_{H} are the Larmor angular frequencies of ^{15}N and ^{1}H respectively, N_{H} is the number of bound protons. The dipolar coupling constant is given by

$$d_{\mathrm{NH}} = -\frac{\mu_0 \hbar \gamma_{\mathrm{H}} \gamma_{\mathrm{N}}}{4\pi \langle r_{\mathrm{CN}}^3 \rangle},$$

where μ_0 is the magnetic constant or vacuum permeability, $\hbar$ is the reduced Planck constant, γ_{N} and γ_{H} are the gyromagnetic constants of ^{15}N and ^{1}H, respectively. Average cubic length is $\langle r_{\mathrm{CN}}^3 \rangle \approx$ and the chemical shift anisotropy is $\Delta\sigma \approx 160 * 10^{-6}$ for N-H bonds in proteins [**?**].

Spectral density $J(\omega)$ is the Fourier transformation of the second order rotational correlation function for N-H bond

$$J(\omega) = 2\int_0^\infty C(t)\cos(\omega t)\mathrm{d}t. \tag{4}$$

The second order rotational correlation is defined as

$$C(t) = \langle (3\cos^2\theta_{t';t'+t} - 1)/2 \rangle_{t'}, \tag{5}$$

where average is ensemble average and θ is the angle between

* samuli.ollila@helsinki.fi; Department of Neuroscience and Biomedical Engineering, Aalto University

N-H bonds at times t' and $t'+t$. The rotational correlation function for protein tumbling in solution contains information about overall rotation of the molecule as well as internal relaxation processes. Assuming that these are independent, the rotational correlation function can be written as [**?**]

$$C(t) = C_I(t)C_O(t), \tag{6}$$

where $C_I(t)$ and $C_O(t)$ are correlation functions for internal and overall rotiations, respectively. Correlation function for fully anisotropic overall rotation can be written as a sum of five exponentials [**?**]

$$C_O(t) = \sum_{j=1}^{5} A_j e^{-t/\tau_j}, \tag{7}$$

where time constants τ_j are related [6] to the diffusion constants around three principal axes of a molecule D_{xx}, D_{yy} and D_{zz}, defined as

$$\begin{aligned} \langle(\Delta\alpha_{t';t'+t})^2\rangle_{t'} &= 2D_{xx}t \\ \langle(\Delta\beta_{t';t'+t})^2\rangle_{t'} &= 2D_{yy}t \\ \langle(\Delta\gamma_{t';t'+t})^2\rangle_{t'} &= 2D_{zz}t, \end{aligned} \tag{8}$$

where $\langle(\Delta\alpha_{t';t'+t})^2\rangle_{t'}$, $\langle(\Delta\beta_{t';t'+t})^2\rangle_{t'}$ and $\langle(\Delta\gamma_{t';t'+t})^2\rangle_{t'}$ are mean square angle deviations of protein intertia axes. The internal correlation function decays to a plateau, which defines the square of order parameter respect to molecular axes S^2. The effective internal correlation time can be defined with the help of reduced correlation function $C_I'(t) = (C_I - S^2)/(1-S^2)$ [**?**]

$$\tau_{\text{eff}} = \int_0^\infty C_I'(t)\mathrm{d}t. \tag{9}$$

Standard analyses of experimental relaxation data usually assume fully or axially isotropic overall rotational motion and single decay constant for interal motion. Then the free parameters (S^2, τ_j, A_j) are fit against spin relaxation data from experiments. This gives most likely very good results for isotropic molecules for which the assumption of single internal motional timescale is reasonable. However, for molecules with significant shape anisotropy or several timescales in internal motions the amoount parameters to be fitted becomes large compared with the typical amount of experimental points.

B. Rotational dynamics from molecular dynamics simulations

Classical molecular dynamics simulations give trajectories of individual atoms as a function of time, which can be used to calculate rotational correlation functions for each bond and explicit separation of internal and overall rotational motions of molecules. The rotational correlation functions can be used to calculate spin relaxation times through Eqs. 1-4, which can be then compared to the experimental data in order to assess simulation model quality [**?**] and interpret experiments [**?**]. However, the comparison is often complicated by the short simulation times [**?**] and incorrect overall rotational diffusion due to water models [**?**]. These issues have been typically overcame by introducing isotropic rotational diffusion term in the correlation functions [**?**] or comparing order parameters instead of spin relaxation rates [**?**]. These approaches are not, however, useful for anitropic proteins and order parameter comparison is not direct comparison between simulations and experiments in the case of freely rotating molecules.

Method presented here can be applied also to anisotropic proteins simulated with timescales routinely accessible with state of the art computational infrastructure. The key idea of the method is to calculate the rotational diffusion constants and then use Eq. 7 to determine the correlation function related to the overall rotational diffusion.

Here we present method to analyse rotational dynamics, The analysis of rotational dynamics permormed in this work can be divided in essentially six steps listed here.
1) Total rotational correlation functions $C(t)$ for protein N-H bonds are calculated from MD simulation trajectory by applying Eq. 5.
2) Rotational correlation functions for internal dynamics $C_I(t)$ are calculated from a trajectory from where the overall rotation of protein is removed.
3) The overall and internal motions are assumed to be independent and overall rotational correlation function is calculated as $C_O(t) = C(t)/C_I(t)$ according to Eq. 6.
4) The protein axes of inertia and their mean square deviations as function of time are calculated from MD simulation trajectory.
5) Rotational diffusion constants D_x, D_y and D_z are calculated by fitting a straight line to mean square angle deviations of inertia axes according to Eq. 8.
6) Timescales in Eq. 7 are calculated from diffusion constants and weighting factors A_j are determined by fitting the equation to rotational correlation functions of overall rotational motion $C_0(t)$ determined in step 3).
7) New total rotational correlation functions $C_N(t)$ are determined by multiplying internal correlation function $C_I(t)$ from step 2) by Eq. 7 with parameters from step 6). Rotational diffusion constants (and τ_i values in Eq. 7) can be also divided by a scaling factor at this point to tune overall rotational diffusion in rotational dynamics model close to experimental value.

C. Simulation and analysis details

Simulations were ran using Gromacs 5 [7] And Amber ff99SB- ILDN [8] force field for proteins . The proteins were solvated to tip3p[9], tip4p [9] or OPC4 [10] water models. NMR structures from [**?**] and [11] are used as initial structure for PaTonB and HpTonB-92, respectively. Temperature was coupled to desired value with v-rescale thermistat [12] and pressure was isotropically set to 1 bar using Parrinello-Rahman barostat [13]. Timestep was 2 fs, Lennart-Jones interactions were cut-off at 1.0 nm, PME [14, 15] was used for electrostatics and LINCS was used to constraint all bond

lengths [16]. Simulation trajectory and related files are available at [??]. The simulated systems are listed in Table I

The rotation is removed by using fit option in *gmx trjconv* and rotational correlation functions are calculated with *gmx rotacf* [17]. Intertia axes of protein are calculated with *compute_inertia_tensor* from MDTraj python library [18]. The spectral density was calculated by first fitting the sum of 471 exponentials having correlation times from 1 ps and 50 ns with logarithmic spacing to the new correlation function

$$C_N(t) = \sum_{i=1}^{N} \alpha_i e^{-t/\tau_i}, \tag{10}$$

by using the *lsqnonneg* routine in MATLAB [19]. The Fourier transform is then calculated by using analytical function for the sum of exponentials

$$J(\omega) = 4 \sum_{i=1}^{N} \alpha_i \frac{\tau_i}{1+\omega^2\tau_i^2}. \tag{11}$$

Similar approach is used previously for lamellar systems in combination with solid state NMR experiements [20, 21].

III. RESULTS AND DISCUSSION

A. Global rotational dynamics of protein

Mean square angle deviations of protein intertia axes as a function of time from PsTonB simulations are shown in Fig. 1. Diffusion coefficients are calculated from linear fits by taking into account lag times less than hundredth of the total simulation length, which is expected to give good statistics for rotation of single molecules in MD simulations [**?**]. Linear diffusion fit to mean square angle displacement seems farily good in Fig. 1, however, log-log plot shown in 8 reveals some anomalous diffusion behaviour at time scales below 0.12 ns. Here we use diffusion coeffiecents to include protein overall motion in spin relaxation calculations and the effect of small anymaly with short timescales is beyond the scope of the work.

The results for diffusion constants from different simulations shown in Table I are in line with previous results from experiments [**?**] and simulations [**?**] for more isotropic proteins. As expected, rotational diffusion is faster in simulations with higher temperature or smaller protein. Also the larger diffusion constants for simulations with tip3p are expected due to the low viscosity of the model [**?**].

Inclusion of rotational diffusion coefficients in N-H bond rotational correlation functions is exemplified in in Fig. 2 for residue 331 located in alpha helix of PaTonB protein. The same analysis is performed also to other bonds and the resulting correlation functions are used to calculate spin relaxation rates. As expected, the N-H bond correlation functions calculated from original MD trajectories shown in Fig. 2 A) decay to fluctuate approximately around zero after ∼20ns. Fluctuations from ideal relaxation behaviour begin already

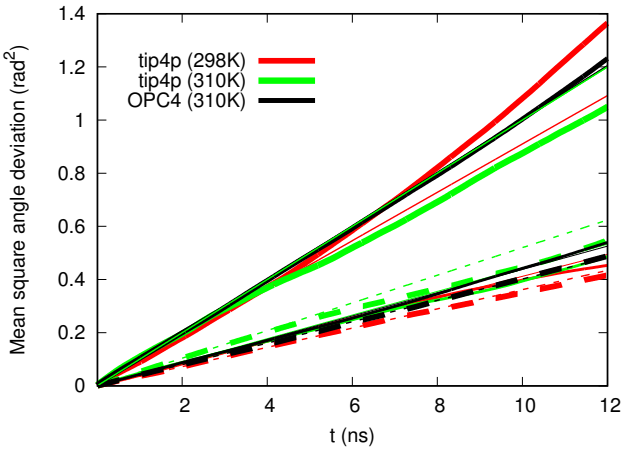

FIG. 1. The intertia tensor angles as a function of time and mean square angular deviations for PsTonB simulation with OPC water model.

close to one hundredth of total simulation time (approximately 4-12ns for the studied systems), which is expected to be the limit for good statistic for rotational dynamics analyzed from single molecule MD simulation [**?**]. Internal correlation functions, calculated from trajectory with overall protein rotation removed, in Fig. 2 B) show rapid decay to a plateau value, which defines the square of the order parameter S^2. The global rotational correlation functions calculated as $C_O(t) = C(t)/C_I(t)$ are shown in Fig. 2 C).

Overall rotational correlation functions were fit to Eq. 7, where timescales for anisotropic rotation [6] were determined by using rotational diffusion constants from Table I, to determine the prefactors A_j for all residues. Resulst for such fit are exemplified with dashed lines in Fig. 2 C) for residue 331 of PsTonB. The prefactors, global rotational timescales and correlation functions for internal relaxation were used to determine new correlation function $C_N(t) = C_I(t)\sum_{j=1}^{5} A_j e^{-t/\tau_j}$, where internal correlation comes directly from MD simulation and global rotational correlation function from diffusion coefficients calculated from MD and Eq. 7. The new correlation functions are exemplified with dashed lines in Fig. 2 A) for residue 331 of PsTonB.

B. Global rotational dynamics in simulations and experiments

Spin relaxation rates were calculated from MD simulations by using new correlation functions, where global rotational dynamics is described by Eq. 7 with timescales from diffusion constants in Table I and prefactors fit to the MD simulation data. The results for PaTonB and HpTonB simulations with different water models are shown in Figs. 3 and **??**, respectivelty.

For PaTonB T_1 and T_1/T_2 ratio are slightly underestimated systemically in all simulations. For HpTonB tip4p gives good agreement with experiments but tip3p results are significantly off. Underestimation of T_1/T_2 ratio suggests that the global

TABLE I. Simulated systems and rotational diffusion coefficients (rad$^2 \cdot 10^7$/s) calculated from simulations.

Protein	Water model	T (K)	$t_{\rm sim}$ (ns)	$t_{\rm anal}$ (ns)	D_{xx}	D_{yy}	D_{zz}	$D_{||}/D_{+}$	D_{av}	files
PaTonB	tip4p	298	400	390	1.81 ± 0.01	2.06 ± 0.03	4.55 ± 0.03	2.35 ± 0.04	2.80 ± 0.02	[**?**]
PaTonB	tip4p	310	400	390	2.60 ± 0.02	2.22 ± 0.05	5.0 ± 0.1	2.07 ± 0.09	3.26 ± 0.07	[**?**]
PaTonB	OPC4	310	1200	1190	2.01 ± 0.01	2.19 ± 0.01	5.01 ± 0.03	2.39 ± 0.02	3.07 ± 0.01	[**?**]
HpTonB-92	tip3p	310	570	370	8.25 ± 0.05	7.67 ± 0.06	15.9 ± 0.3	1.99 ± 0.06	10.6 ± 0.2	[**?**]
HpTonB-92	tip3p	303	800	790	6.24 ± 0.02	7.04 ± 0.03	11.9 ± 0.2	1.80 ± 0.03	8.40 ± 0.07	[**?**]
HpTonB-92	tip4p	310	470	370	3.6 ± 0.1	3.24 ± 0.01	6.3 ± 0.3	1.8 ± 0.1	4.4 ± 0.2	[**?**]
HpTonB-92	tip4p	303	400	200	2.7 ± 0.1	2.71 ± 0.02	5.6 ± 0.5	2.1 ± 0.2	3.7 ± 0.2	[**?**]
HpTonB-92	OPC4	310	800	790	2.85 ± 0.01	2.70 ± 0.01	5.56 ± 0.01	2.00 ± 0.01	3.70 ± 0.01	[**?**]

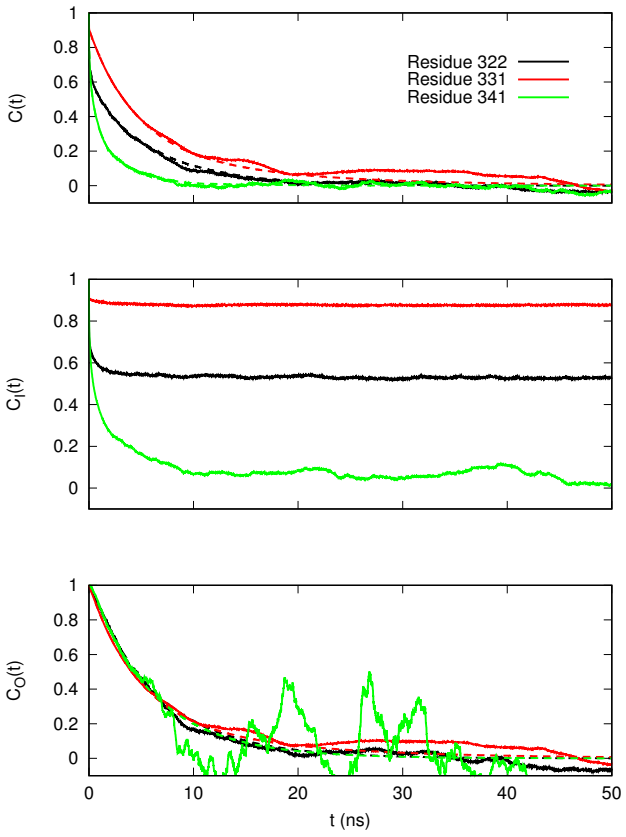

FIG. 2. Example correlation functions for residue 331 of PsTonB calculated from MD simulations with different water models. A) total correlation functions $C(t)$ calculated from MD simulation (solid lines) and new correlation functions determined from Eqs. 6 and 7 by using rotational diffusion constants and fitted prefactors (see section II B) (dashed lines), B) correlation function for internal motions and C) correlation function for overall motions determined from Eq. 6 ($C_O(t) = C(t)/C_I(t)$) (solid lines) and fits to Eq. 7.

rotational diffusion is overestimated in simulations [**?**]. Thus, we tested if scaling of diffusion coefficients with constant factor gives better agreement with experiments. Rotational diffusion coefficients for PaTonB simulation with tip4p and HpTonB simulation with tip3p were first divided by factors 1.2 and 2.9, respectively. Then, the new correlation functions $C_N(t)$ were calculated by using timescales determined from scaled diffusion constants and prefactors from the fit to the overall correlation functions. The spin relaxation results from these correlation functions are shown in Figs. 5 and 6 for PsTonB and HpTonB, respectively, are in good agreement with experiments. This suggests that the new correlation functions with the scaled diffusion coefficients can be used to interpret the protein rotational dynamics from NMR relaxation data.

The rotational diffusion coefficients after the scaling are shown in Table II. These diffusion constants applied in the global rotational correlation functions give spin relaxation times in good agreement with experiments, thus these can be considered as an interperation of NMR relaxation data. The diffusion coefficients from tip3p simulation for HpTonB-92 with scaled diffusion constants (Table II) and slightly smaller than diffusion coefficients from tip4p simulation (Table I), which also gave a relatively good agreement with experiments. However, the scaled results from tip3p simulation gives slighltly better agreement for T_1/T_2 ratio and, thus, a better interpretation for experiments.

TABLE II. Rotational diffusion coefficients scaled with constant factor which gives a good agreement for spin relaxation data, 2.9 for tip3p simulation of HpTonB and by 1.2 for tip4p simulation of PsTonB.

	HpTonB-92	PsTonB
D_{xx}	2.15 ± 0.01	1.51 ± 0.01
D_{yy}	2.43 ± 0.01	1.72 ± 0.03
D_{zz}	4.10 ± 0.01	3.79 ± 0.03
D_{av}	2.90 ± 0.03	2.3 ± 0.02
τ_c(ns)	5.7 ± 0.1	7.2 ± 0.1

C. Interpretation of protein internal relaxation from MD simulations

Spin relaxation rates from tip4p simulations for PsTonB are in good agreement with experimetns (see Figs **??**), thus the simulations can be used to give interpretation for rotational

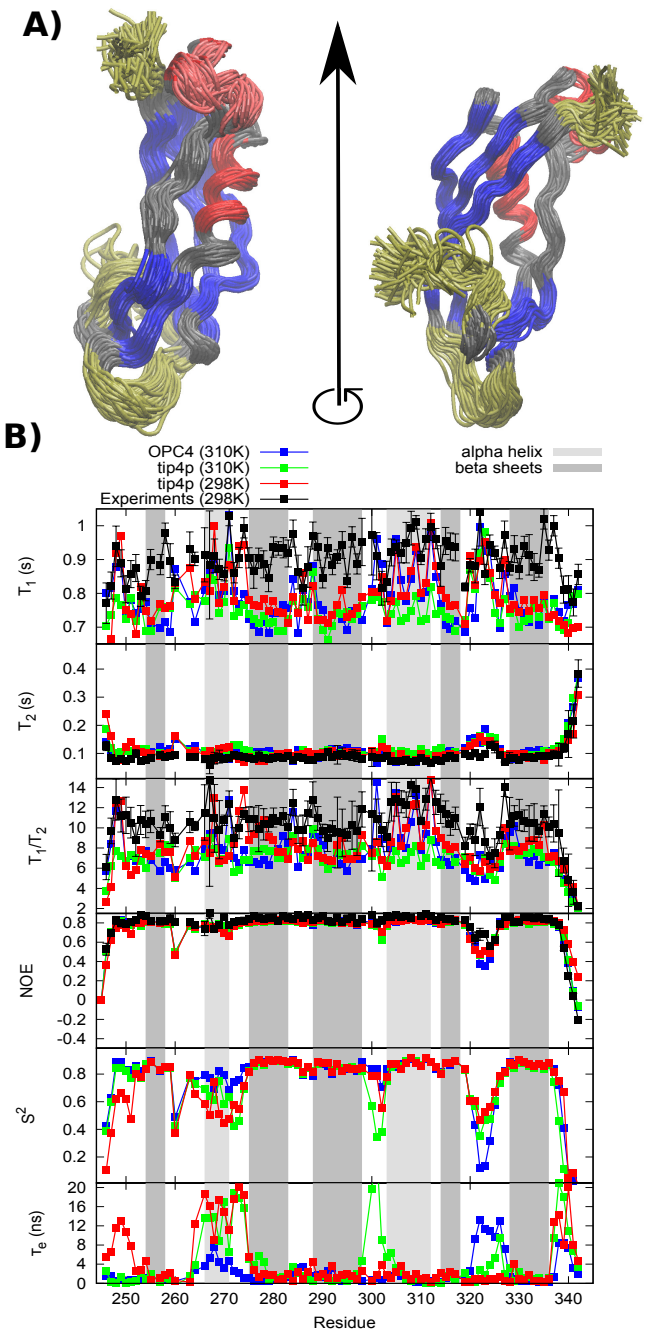

FIG. 3. A) Structures sampled by PsTonB from MD simulations (100 structures from 400ns long trajectory). Alpha helixces are shown with red, beta sheets with blue and residues 246-251, 320-326 and 338-342 with increased internal dynamics are colored yellow. Alphahelix sampling between two orientations (residues 266-270) is shown with pink in left column. B) Spin relaxation rates, order parameters and effective internal correlation times from experiments and simulations.

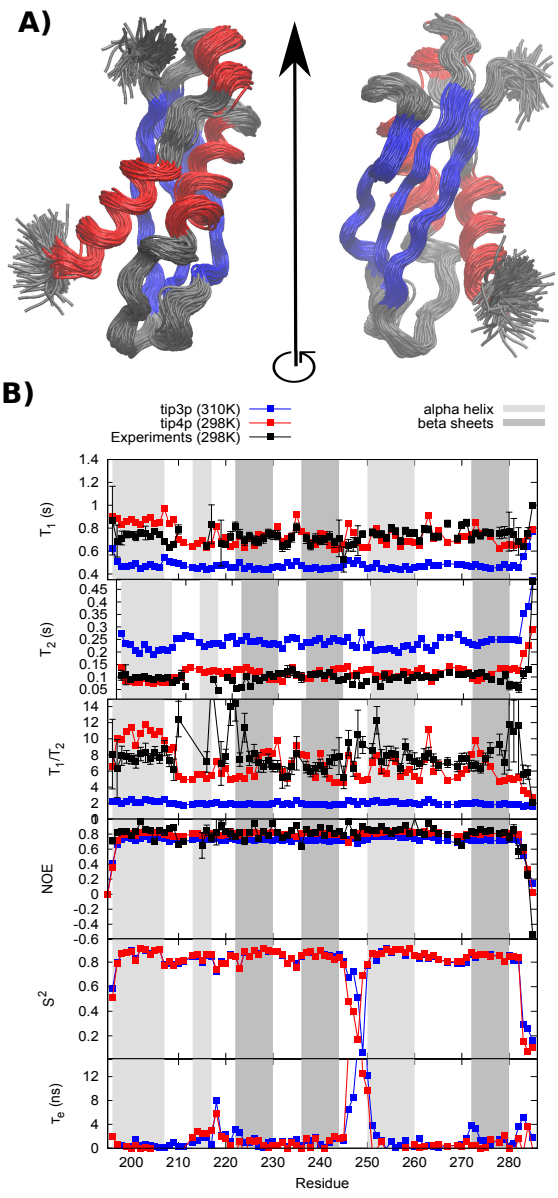

FIG. 4. Relaxation parameters for HpTonB short construct from experiments and simulations with Amber-ildn and different water models

relaxation processes in proteins, which correspond the NMR relaxation results. Spin relaxation rate deviations from baseline are observed for residues 246-251 in N-terminus, residues 320-326 and residues 338-342 in C-terminus. These segments are coloured in yellow in Fig. **??** A), which already revels ecnhanged conformational sampling in these regions. Also order parameters are low and effective internal relaxation times long for these segements as seen in Fig. **??** B).

More detailed interpretation of different relaxation processes experienced by different residues can be done by analysing timescales which leads in simulation model to the spin relaxation rates in agreement with experiments. Prefactors from Eq. **??** fitted in rotational correlation functions in agreement with spin relaxation data are shown in Fig 7 for different residues in PsTonB. Residue 331 represents the last alpha helix before C terminus and its rotational relaxation is mostly dominated by relaxations with timescales $\sim$5.5 ns and $\sim$8 ns, which arise from global rotation of protein an only

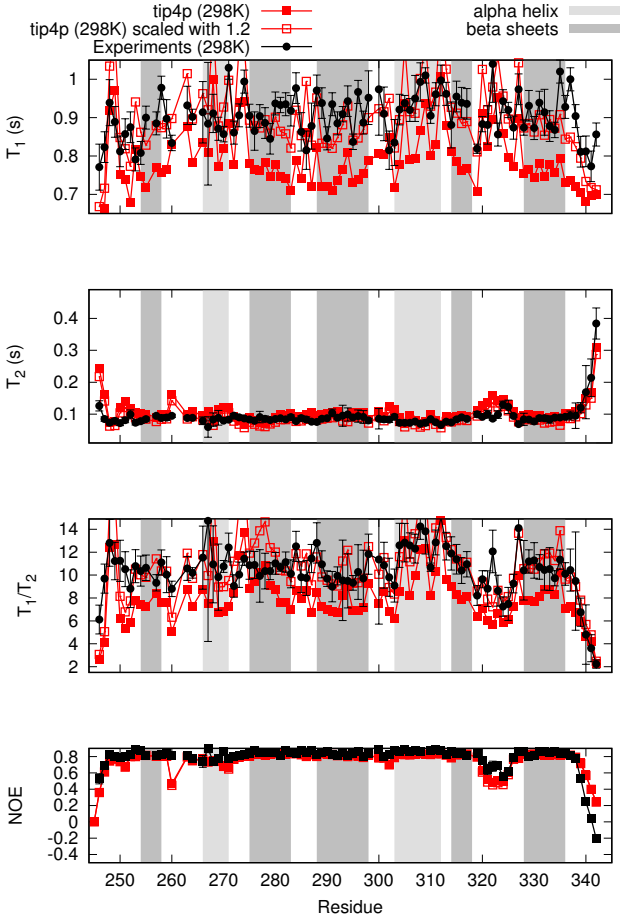

FIG. 5. Relaxation parameters for PsTonB from experiments and simulations with Amber-ildn and different water models. Overall rotational diffusion corrected with factor 1.2.

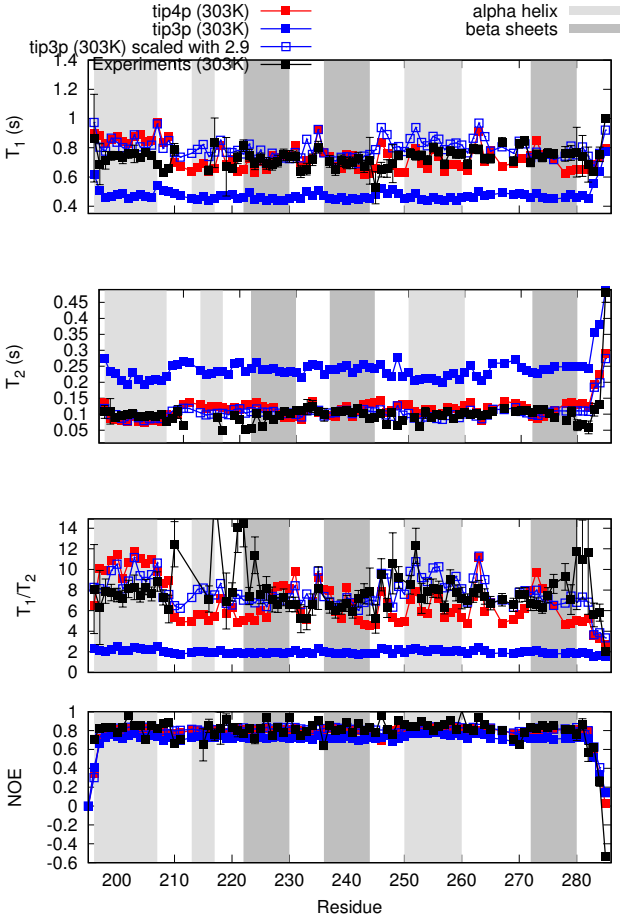

FIG. 6. Relaxation parameters for HpTonB short construct from experiments and simulations with Amber-ildn and different water models

small fraction of relaxation arises from fast internal motions, in accordance with large order parameter value (??). Relaxation of residue 322 is also dominated by relaxation processes with timescale around ∼8 ns, but fast motions related to internal protein dynamics are more significant than for alpha helix residue 331. This explains the low order parameter (??) measured small NOE and large T_2 relaxation times values shown in Fig. **??**. Rotational dynamics of residue 341 located in N terminus is dominated by the fast motions related to the internal protein relaxation, as expected from the low order parameter. The contribution from timescales close to ∼13 ns are probably related to slower conformational sampling of the N terminus, which is also seen in sampled conformations and large effective correlation times in Fig. **??**.

In addition, low order parameters and larger effective correlation times are observed for PsTonB residues 260-274 and 300-303 in Fig. 3 B). For residues 260-274 this can be explained by two different orientations sampled by alpha helix on that region, as highlighted with pink in Fig. 3 A). This explains also the lower resolution in NMR spectra observed for this and similar region in HpTonB structures [**?**]. Low order parameters and large effective correlation times between

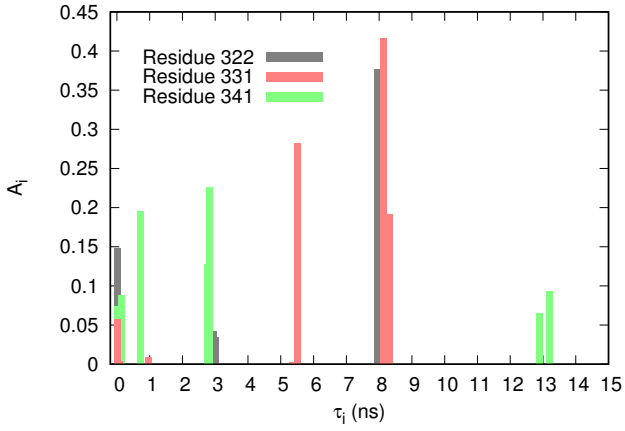

FIG. 7. Prefactors A_i corresponding different timescales τ_i in Eq.**??** resulting from a fit in correlation functions giving good agreement with spin relaxation rates in experimetns for PsTonB.

residues 300-303 are not seen in spin relaxation data, thus it is not clear if these arise from simulation artefact.

Spin relaxation rate deviations from baseline are observed only few residues in terminal ends for HpTonB-92 as seen in Fig. **??**. This is the case also in simulations, except that the N terminus flexibility seems to be somewhat overestimated and low order parameters and long effetive correlation times are also observed for residues 245-250. The latter observation probably arises (at least partly) from simulation artefacts because deviation form experimental relaxation data is relatively large for these residues. More detailed discussion together with longer HpTonB construct is presented elsewhere [**?**].

IV. CONCLUSIONS

Rotation of protein intertia axes is observed to experience linear diffusion behaviour and overall diffusion component of rotational correlation functions of individual N-H bonds can can be successfully fitted to the model assuming anitropic diffusion for whole molecule.

Rotational diffusion of whole molecules is overestimated by a factor of ∼3 in simulations with tip3p water, in agreement with previous studies [**?**]. The simulations with tip4p and opc4 water models give more realistic diffusion coefficients, which overestimate diffusion only with factors ∼1-1.2.

The overstimated overall diffusion coefficient can be corrected post-simulationally to compare internal dynamics and order with experiments.

The presented methodology can be used to interpret spin relaxation experiments by using MD simulations [**?**] and asses the quality of protein force fields against NMR experiments. The presented scaling of overall anisotropic diffusion allows this also for simulations with incorrect rotational diffusion due to water models, which is the case in simulations with tip3p.

ACKNOWLEDGMENTS

[1] V. A. Jarymowycz and M. J. Stone, Chemical Reviews **106**, 1624 (2006).

[2] D. Korzhnev, M. Billeter, A. Arseniev, and V. Orekhov, Progress in Nuclear Magnetic Resonance Spectroscopy **38**, 197 (2001).

[3] .

[4] A. Abragam, *The Principles of Nuclear Magnetism* (Oxford University Press, 1961).

[5] L. E. Kay, D. A. Torchia, and A. Bax, Biochemistry **28**, 8972 (1989).

[6] $\tau_1 = (4D_{xx} + D_{yy} + D_{zz})^{-1}$, $\tau_2 = (D_{xx} + 4D_{yy} + D_{zz})^{-1}$, $\tau_3 = (D_{xx} + D_{yy} + 4D_{zz})^{-1}$, $\tau_4 = [6(D + (D^2 - L^2)^{-1/2}]^{-1}$, $\tau_5 = [6(D - (D^2 - L^2)^{-1/2}]^{-1}$, $D = \frac{1}{3}(D_{xx} + D_{yy} + D_{zz})$ and $L^2 = \frac{1}{3}(D_{xx}D_{yy} + D_{xx}D_{zz} + D_{yy}D_{zz})$.

[7] M. J. Abraham, T. Murtola, R. Schulz, S. Pll, J. C. Smith, B. Hess, and E. Lindahl, SoftwareX **12**, 19 (2015).

[8] K. Lindorff-Larsen, S. Piana, K. Palmo, P. Maragakis, J. L. Klepeis, R. O. Dror, and D. E. Shaw, Proteins: Structure, Function, and Bioinformatics **78**, 1950 (2010).

[9] W. L. Jorgensen, J. Chandrasekhar, J. D. Madura, R. W. Impey, and M. L. Klein, J. Chem. Phys. **79**, 926 (1983).

[10] S. Izadi, R. Anandakrishnan, and A. V. Onufriev, The Journal of Physical Chemistry Letters **5**, 3863 (2014).

[11] A. Ciragan, A. S. Aranko, I. Tascon, and H. Iwa, Journal of Molecular Biology **428**, 4573 (2016).

[12] G. Bussi, D. Donadio, and M. Parrinello, J. Chem. Phys. **126** (2007).

[13] M. Parrinello and A. Rahman, J. Appl. Phys. **52**, 7182 (1981).

[14] T. Darden, D. York, and L. Pedersen, J. Chem. Phys. **98**, 10089 (1993).

[15] U. L. Essman, M. L. Perera, M. L. Berkowitz, T. Larden, H. Lee, and L. G. Pedersen, J. Chem. Phys. **103**, 8577 (1995).

[16] B. Hess, J. Chem. Theory Comput. **4**, 116 (2008).

[17] M. Abraham, D. van der Spoel, E. Lindahl, B. Hess, and the GROMACS development team, *GROMACS user manual version 5.0.7* (2015).

[18] R. T. McGibbon, K. A. Beauchamp, M. P. Harrigan, C. Klein, J. M. Swails, C. X. Hernández, C. R. Schwantes, L.-P. Wang, T. J. Lane, and V. S. Pande, Biophysical Journal **109**, 1528 (2015).

[19] .

[20] A. Nowacka, N. Bongartz, O. Ollila, T. Nylander, and D. Topgaard, J. Magn. Res. **230**, 165 (2013).

[21] T. M. Ferreira, O. H. S. Ollila, R. Pigliapochi, A. P. Dabkowska, and D. Topgaard, J. Chem. Phys. **142**, 044905 (2015).

SUPPLEMENTARY INFORMATION

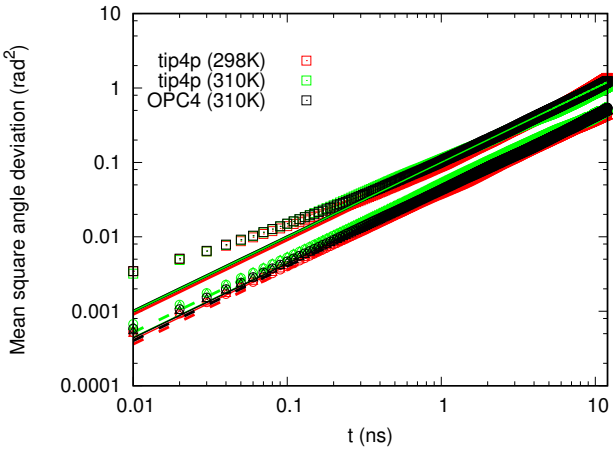

FIG. 8. The intertia tensor angles as a function of time and mean square angular deviations for PsTonB simulation with OPC water model.